A Communication Theoretical Analysis of Synaptic Multiple-Access Channel in Hippocampal-Cortical Neurons

Derya Malak, *Student Member, IEEE,* and Ozgur B. Akan, *Senior Member, IEEE*

***Abstract*—Communication between neurons occurs via transmission of neural spike trains through junctional structures, either electrical or chemical synapses, providing connections among nerve terminals. Since neural communication is achieved at synapses, the process of neurotransmission is called synaptic communication. Learning and memory processes are based on the changes in strength and connectivity of neural networks which usually contain multiple synaptic connections. In this paper, we investigate multiple-access neuro-spike communication channel, in which the neural signal, i.e., the action potential, is transmitted through multiple synaptic paths directed to a common postsynaptic neuron terminal. Synaptic transmission is initiated with random vesicle release process from presynaptic neurons to synaptic paths. Each synaptic channel is characterized by its impulse response and the number of available postsynaptic receptors. Here, we model the multiple-access synaptic communication channel, and investigate the information rate per spike at the postsynaptic neuron, and how postsynaptic rate is enhanced compared to single terminal synaptic communication channel. Furthermore, we analyze the synaptic transmission performance by incorporating the role of correlation among presynaptic terminals, and point out the postsynaptic rate improvement.**

***Index Terms*—Synaptic multiple-access channel, neuro-spike communication, synapse, achievable rate.**

I. Introduction

MOLECULAR communication is a new communication paradigm in which molecules are the information carriers [1]. Some examples of molecular communication mechanisms are calcium signaling [2], pheromones and neurotransmitters [1].

In the literature, different molecular network architectures are proposed to realize the communication between nanomachines that can be deployed over different distances. In [3], flagellated bacteria and catalytic nanomotor techniques are proposed to cover the medium-range. In addition, there are various molecular communications options for short range [4], and long range [5]. Although neural signaling has a long history initiated from the Hodgkin's pioneering work [6], among all molecular communication paradigms, neuro-spike communication that uses the neurotransmitters as information carriers has not been studied to the fullest extent [7].

There are several studies about the physiological principles of the neuron. The axonal propagation in the hippocampal neurons and the reliability of this transmission are investigated in [8]. The vesicle release process, which initiates the synaptic transmission in hippocampal neurons is described [9], [10]. These contributions mediate the analysis of neurons from the perspective of communication theory.

Neuro-spike communication is an interdisciplinary research area, which combines the fields of neuroscience, communications and nanotechnology. The transferred amount of information through a synaptic connection has an important role in learning and memory processes. There has been some research concentrating on the information transmission limits over synaptic terminals [11]. In [7], authors investigate the behavior of neurons as a new nanoscale communication paradigm and model the end-to-end neural communication channel. A synaptic communication model is suggested in [11]. It involves the fundamental events during the synaptic transmission as different blocks, namely the vesicle release in response to a spike, Excitatory PostSynaptic Potential (EPSP), which is the temporary increase in the postsynaptic membrane potential caused by the flow of positively charged ions into the postsynaptic cell due to the vesicle release [12], and trial-to-trial variability of this potential. The authors derive the theoretical lower bounds on the capacity of a simple cortical synapse model by signal estimation and signal detection paradigms. However, the model is based on point-to-point synaptic connections. Furthermore, authors employ univesicular release in the model, and do not consider the variability in vesicle fusion rate on distinct sites of the presynaptic terminal.

In this paper, we investigate the multiple-access communication among hippocampal-cortical neurons occurring via exchange of molecules through chemical synapses, which involve neurotransmitters and are far more common and modifiable compared to electrical synapses that do not involve neurotransmitters [13]. We perform analysis to observe how the postsynaptic rate improves with increasing number of users, i.e., presynaptic terminals. Our main motivation in this work is that learning and memory processes are based on the changes in strength and connectivity of neural networks, which usually contain multiple synaptic connections. Therefore, we specifically focus on the multi-input single-output neuro-

Manuscript received October 21, 2012; revised January 25, 2013. The editor coordinating the review of this paper and approving it for publication was T. Q. S. Quek.

The authors are with the Next-Generation and Wireless Communications Laboratory, Department of Electrical and Electronics Engineering, Koc University, Istanbul, 34450, Turkey (e-mail: {dmalak, akan}@ku.edu.tr).

This work was supported in part by the Turkish Scientific and Technical Research Council Career Award under grant #109E257, and by the Turkish National Academy of Sciences Distinguished Young Scientist Award Program (TUBA-GEBIP), and by IBM through IBM Faculty Award.

Digital Object Identifier 10.1109/TCOMM.2013.042313.120799

spike communication channel characteristics to observe the tradeoff between multiple users and total rate at the output. Synaptic plasticity, i.e., the change in the synaptic connection strengths depending on the presynaptic input strengths and channel parameters, is the main mechanism behind learning and memory. Learning occurs through cooperation between synaptic inputs and the plasticity rules select inputs which have a strong correlation with other inputs [14]. Synaptic plasticity contributes to memory storage, and the activity-dependent development of neuronal networks. Thus, we especially focus on the positive influence of correlation among presynaptic neural spike trains on the communication rate at the postsynaptic neuron.

In this paper, we apply existing techniques in communications to analyze the performance of the neuronal channels. However, we provide a comprehensive mathematical model of the communication channel including the stochastic behavior of the input, the action potential generation, dynamic and stochastic nature of vesicle release process, stochastic nature of the communication channel. Although the point-to-point synaptic channel performance is studied in the literature widely as in [7] and [15], we provide a more comprehensive neuro-spike communication channel model in Section II. Our contributions range from incorporation of the stochastic nature of all the parameters along the communication line into the dynamic nature of processes, including the random nature of the input, the communication channel, the quantal variability, multivesicular release process, pool-based synapse model. In this paper, we develop a rate region analysis for the multiple-access communication channel, and show the boosting effect of the correlation on the sum rate at the channel output. In addition, incorporation of the effect of correlation among presynaptic terminals on the postsynaptic rate is also provided for the first time in the literature. We analytically show that as the correlation increases, the postsynaptic rate is enhanced.

The remainder of this article is organized as follows. In Section II, we provide the linear-nonlinear-Poisson (LNP) model of spike generation, vesicle release and postsynaptic response variability in a link-to-link synaptic communication channel. In Section III, we extend the single-input single-output channel model to a multiple-access synaptic communication channel and obtain the analytical expression for multiuser channel rate regions. In Section IV, we evaluate the performance of the multiple-access synaptic communication channel, quantitatively investigate the total information rate per spike at the postsynaptic neuron for the multiuser communication system, and compare it to a single terminal synaptic channel. We conclude the paper in Section V.

II. Model Description

In this section, we provide the reader with the essential background of neural signaling. Then, stating our methodology, we concentrate on the fundamentals of the single-input single-output (SISO) neuro-spike communication channel.

a) Neural Signaling Background: we provide the essential components of neural signaling. These include *action potential generation*, *neural firing*, *vesicle release*, *postsynaptic potential* and *postsynaptic response variability*.

Action potential is a short-lasting event in which the electrical membrane potential of a cell rapidly rises and falls, following a consistent trajectory [7]. During the action potential, part of the neural membrane opens to allow positively charged ions inside the cell and negatively charged ions out. This process causes a rapid increase in the positive charge of the nerve fiber. When the charge reaches $+40\mathrm{mV}$, the impulse is propagated down the nerve fiber. This electrical impulse is carried down the nerve through a series of action potentials. *Neural firing* is the response of a neuron when it is stimulated. A neuron that emits an action potential is often said to fire.

Synaptic vesicles store neurotransmitters to be released at synapses and constantly reproduced by the cells. These vesicles are essential for conduction of nerve impulses. Action potentials trigger the complete fusion of the synaptic vesicle with the cellular membrane, and then, the excretion from the cell through exocytosis, which is called *vesicle release* [16].

Postsynaptic potential is the membrane potential at the postsynaptic terminal of a chemical synapse. In neuroscience, an EPSP is a temporary depolarization of postsynaptic membrane potential caused by the flow of positively charged ions into the postsynaptic cell as a result of opening of ligand-gated ion channels [12]. An Inhibitory PostSynaptic Potential (IPSP), which is the opposite of an EPSP, makes a postsynaptic neuron less likely to generate an action potential. *Postsynaptic response variability* is the trial-to-trial amplitude variability of the postsynaptic response to a vesicular release.

b) Objectives and Methodology: we aim to analyze the rate region at the postsynaptic terminal when there are multiple presynaptic terminals. Hence, as the initial step to the rate region analysis, in this section, we focus on the SISO synaptic channel characteristics. Therefore, we first explain the firing and spike generation mechanisms. Then, we provide a model for vesicle release from presynaptic terminals, and the model of channel response depending on the trial-to-trial variability in vesicle release process. To characterize the rate region, we need to find the power spectral densities (PSDs) of the signal and noise components at the postsynaptic terminal by incorporating the stochastic characteristics of presynaptic input, neuron terminal, and the synaptic channel parameters. Therefore, in this section, we provide the main blocks and steps for analytically obtaining the PSD at the postsynaptic terminal for the SISO synaptic communication channel, and calculate the statistical parameters, i.e., the means and variances of the random variables denoting the action potential rate, vesicle release processes, quantal variability, which play fundamental roles on the performance of neuro-spike communication.

A. Neuronal Firing: The Soma Channel

In a SISO neuron channel model, when a random stimulus, $m(t)$, is applied to the presynaptic terminal, a spike train, $S(t)$, is generated at its axon which has a time varying neuronal firing rate $\lambda(t)$. In our model, $m(t)$ and $S(t)$ are jointly wide-sense stationary (jointly WSS), implying that both $m(t)$ and $S(t)$ are WSS processes, and the cross correlation function $R_{m,S}(\tau) = \mathrm{E}\left[m(t)S(t+\tau)\right]$ is independent of t for all τ.

1) Low Pass Filtering: The stimulus $m(t)$, which is a wide sense stationary (WSS) process, with bandwidth B_m, and

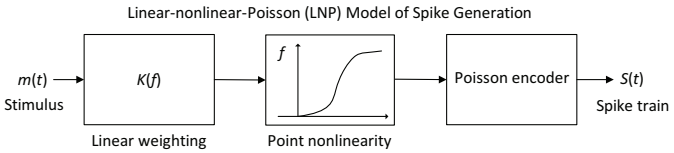

Fig. 1. A functional model of neural spike responses [17]. In [17], a Linear-Nonlinear-Poisson (LNP) model for neural responses is proposed, which has been successfully used to describe the neuronal response characteristics.

autocorrelation function (ACF) $R_m(t+\tau,t)=R_m(\tau)$ enters the hypothetical $k(t)$ filter, which simulates the empirical characteristics of axonal filtering process. We ignore axonal noise for simplicity. Hence, the filter response, i.e., $v(t)$, is

$$v(t)=m(t)*k(t),\ k(t)=\frac{1}{C}\exp\left(-\frac{t}{RC}\right)U(t). \tag{1}$$

$k(t)$ is a low-pass filter denoting axonal response. Hence, $k(t)$ corresponds to the first block of LNP model shown in Fig. 1. The absolute square of the frequency response of $k(t)$ filter is $|K(f)|^2=\frac{R^2}{1+(2\pi fRC)^2}$, which is later utilized in the calculation of the PSD of the generated spike train. Hence, the ACF of $v(t)$, i.e., $R_v(t+\tau,t)=R_v(\tau)$, is obtained as

$$R_v(\tau)=\int_0^\infty\int_0^\infty R_m(\tau-\alpha+\beta)\frac{1}{C^2}\exp\left(-\frac{\alpha+\beta}{RC}\right)\mathrm{d}\alpha\mathrm{d}\beta, \tag{2}$$

which is also a WSS random process since it is obtained by low-pass (linear) filtering of the stimulus $m(t)$, which is a zero mean random process. Hence, the PSD of $v(t)$ is obtained as

$$S_v(f)=|K(f)|^2S_m(f)=\frac{R^2}{1+(2\pi fRC)^2}S_m(f). \tag{3}$$

2) Point (Sigmoidal) Nonlinearity: Point nonlinearity block, the second stage of the LNP model, transforms the linearly weighted input into an inhomogenous spike rate function, which is later utilized in Poisson encoder, the third stage of the LNP model, to generate Poisson impulses [17]. The inhomogeneous spike rate can be determined as $\lambda(t)=f(m(t)*k(t))$, where f is a sigmoidal nonlinearity, and is a scalar and continuous function with nonnegative outputs. In the limit of small time bins, the probability of spike generation becomes $P(\text{Spike})\propto f(m(t)*k(t))$. Considering the number of arrivals in the time interval Δt, given as k, which follows a Poisson distribution with associated parameter $\lambda_{\Delta t}=\int_{\Delta t}\lambda(t)\,\mathrm{d}t$, $Prob(k)=e^{-\lambda_{\Delta t}}\lambda_{\Delta t}^k/k!$. In the limit of very small Δt, $Prob(0)=1-\lambda(t)\Delta t$. Hence, the spike generation probability is given as $P(\text{Spike})=\lambda(t)\Delta t$, which is proportional to $\lambda(t)$.

The sigmoidal nonlinearity function is given as

$$f\left(v(t)\right)=\left(1+\exp\left(-a\left(v(t)-v_{1/2}\right)\right)\right)^{-1}, \tag{4}$$

which is a mapping on $v(t)$ and depends on the constant parameters a and $v_{1/2}$. In [18], authors model the spike rate for cortical neurons of a monkey, and the sigmoidal nonlinearity curve is fitted with the parameters $a=\frac{1}{0.029^\circ}$ and $v_{1/2}=0.036^\circ$ and scaled with $\lambda_{\max}=36.03$ Hz. These parameters are also applicable to our analysis.

The sigmoidal nonlinearity is a result of the saturation of presynaptic neurons. As the firing rate increases, the synaptic channel is saturated with available vesicles in the docked pool. Hence, the number of available vesicles in the docked pool decreases. In this paper, the neuronal firing rate should be high enough to avoid zero throughput. Furthermore, we assume that the synaptic channel could be saturated. However, to simplify the analysis, we approximate the nonlinear model about the non-saturated region of the sigmoidal curve by linearizing the sigmoidal function around $f(v(t))=0.5\lambda_{\max}$, where $v(t)=v_{1/2}$. Hence, we can approximate $f(v(t))$ as

$$f(v)=\begin{cases}0 & \text{if } v(t)\le v_{1/2}-\frac{2}{a}\\ \lambda_{\max}\left(\frac{1}{2}+\frac{a\left(v-v_{1/2}\right)}{4}\right) & \text{if } \left|v(t)-v_{1/2}\right|\le\frac{2}{a}\\ \lambda_{\max} & \text{if } v(t)\ge v_{1/2}+\frac{2}{a}\end{cases}, \tag{5}$$

where $f(v_{1/2}-\frac{2}{a})\approx 0.12\lambda_{\max}$, and $f(v_{1/2}+\frac{2}{a})\approx 0.88\lambda_{\max}$. Therefore, linearizing the output of the sigmoidal nonlinearity block, we obtain

$$\lambda(t)=\lambda_{\max}\left(\frac{2-av_{1/2}}{4}+\frac{av(t)}{4}\right)P\left(|v(t)-v_{1/2}|\le\frac{2}{a}\right)+\lambda_{\max}P\left(v(t)-v_{1/2}\ge\frac{2}{a}\right), \tag{6}$$

where the rate of the Poisson spike generation process changes linearly, provided that $v_{1/2}-\frac{2}{a}\le v(t)\le v_{1/2}+\frac{2}{a}$. When $v(t)\ge v_{1/2}+\frac{2}{a}$, the neuron is saturated and $\lambda(t)=\lambda_{\max}$. Hence, the mean firing rate can be determined as

$$\bar{\lambda}=\mathrm{E}\left[\lambda\right]=\lambda_{\max}\left(\frac{2-av_{1/2}}{4}\right)P\left(|v(t)-v_{1/2}|\le\frac{2}{a}\right)+\lambda_{\max}P\left(v(t)-v_{1/2}\ge\frac{2}{a}\right). \tag{7}$$

We assume that the stimulus to each presynaptic terminal is normal distributed with zero mean and variance σ^2. Hence,

$$P\left(|v(t)-v_{1/2}|\le\frac{2}{a}\right)=\frac{1}{2}\left[\mathrm{erf}\left(\frac{g^{-1}\left(\frac{2}{a}+v_{1/2}\right)}{\sigma\sqrt{2}}\right)+\mathrm{erf}\left(\frac{g^{-1}\left(\frac{2}{a}-v_{1/2}\right)}{\sigma\sqrt{2}}\right)\right] \tag{8}$$

$$P\left(v(t)-v_{1/2}\ge\frac{2}{a}\right)=\frac{1}{2}\left[1-\mathrm{erf}\left(\frac{g^{-1}\left(\frac{2}{a}+v_{1/2}\right)}{\sigma\sqrt{2}}\right)\right],$$

where $g(m(t))=m(t)*k(t)$ is a function of the stimulus, and we assume that $g(.)$ is one-to-one. Hence, the inverse of g, denoted by g^{-1}, is the unique function with domain equal to the range of g that satisfies $g\left(g^{-1}(x)\right)=x$ for all x in the range of g. Furthermore, as we assume $v(t)\ge v_{1/2}-\frac{2}{a}$ (to prevent firing rate from being zero), we scale the probabilities in (8) so that they add up to 1. From (6), (7) and (8), we get

$$\lambda(t)=\bar{\lambda}+\bar{\lambda}bv(t), \tag{9}$$

where $b=\frac{a\lambda_{\max}}{4\bar{\lambda}}P\left(|v(t)-v_{1/2}|\le\frac{2}{a}\right)$. Using (9), the ACF of $\lambda(t)$ can be determined as $R_\lambda(\tau)=\bar{\lambda}^2\left(1+b^2R_v(\tau)\right)$. Hence, the autocovariance function of $\lambda(t)$ can be obtained

by subtracting $\bar{\lambda}^2$ from $R_\lambda(\tau)$ as $C_\lambda(\tau) = \bar{\lambda}^2 b^2 R_v(\tau)$. The variance of the spike rate, i.e., $\sigma_\lambda^2 = C_\lambda(0)$, is obtained as

$$\sigma_\lambda^2 = \bar{\lambda}^2 b^2 R_v(0) = \bar{\lambda}^2 b^2 {\sigma_v}^2, \tag{10}$$

where ${\sigma_v}^2$ is the variance of $v(t)$, which is a zero mean WSS process. Using (7) and (10), the coefficient of variation, i.e., the contrast of firing rate, for the spike train can be found as

$$c_\lambda = \sigma_\lambda / \bar{\lambda} = b\sigma_v. \tag{11}$$

3) Poisson Encoding: The Poisson spike train at the output of the presynaptic neuron axon, $S(t)$, can be formulated as

$$S(t) = \sum_{i=1}^{N} \delta(t - t_i) = \frac{d}{dt} \sum_{i=1}^{N} u(t - t_i) = \frac{dN(t)}{dt},$$

where $N(t)$ models an inhomogeneous, i.e., non-constant rate, Poisson arrival process characterized with rate parameter $\lambda(t)$, which is the expected number of arrivals that occur per unit time. The mean of this Poisson arrival process is $\mathrm{E}[N(t)] = \int_0^t \lambda(\tau)\,\mathrm{d}\tau$. Hence, the average rate for spike generation at the presynaptic terminal is

$$\lambda(t) = \langle S(t) \rangle = \mathrm{E}[S(t)] = \frac{d\mathrm{E}[N(t)]}{dt}. \tag{12}$$

The ACF $R_S(t,s)$ of the spike train, which is an inhomogeneous Poisson process with rate $\lambda(t)$, can be calculated using the ACF of the Poisson spike process, i.e., $R_N(t,s)$, as

$$\begin{aligned} R_S(t,s) &= \frac{\partial}{\partial t}\left[\frac{\partial R_N(t,s)}{\partial s}\right] \\ &= \begin{cases} \frac{\partial}{\partial t}\left[\lambda(s)\int_0^t \lambda(\eta)\,\mathrm{d}\eta + \lambda(s)\right] & \text{if } t > s \\ \frac{\partial}{\partial t}\left[\lambda(s)\int_0^t \lambda(\eta)\,\mathrm{d}\eta\right] & \text{if } t < s \end{cases} \\ &= \bar{\lambda}^2 + \bar{\lambda}^2 b(v(t) + v(s)) + (\bar{\lambda}b)^2 v(t)v(s) \\ &+ (\bar{\lambda} + \bar{\lambda}bv(s))\delta(t-s). \end{aligned} \tag{13}$$

However, $R_S(t,s)$ is not a WSS random process. Therefore, it does not make sense to talk about its power spectrum. Hence, we assume that the process is ergodic, and take its expectation. The expectation can be replaced by the limit of a time average. Then, we calculate the autocorrelation of time averaged process using the result (13), which we interpret as

$$R_{\bar{S}}(t,s) = \bar{\lambda}^2 + (\bar{\lambda}b)^2 R_v(t-s) + \bar{\lambda}\delta(t-s), \tag{14}$$

which is a WSS process, and we can rewrite (14) as

$$R_{\bar{S}}(\tau) = \bar{\lambda}^2 + (\bar{\lambda}b)^2 R_v(\tau) + \bar{\lambda}\delta(\tau), \tag{15}$$

of which we can talk about the power spectrum. The PSD of $R_{\bar{S}}(\tau)$, thus, can be found as

$$S_{\bar{S}}(f) = \bar{\lambda} + \left(\bar{\lambda}b\right)^2 |K(f)|^2 S_m(f) + \bar{\lambda}^2\delta(f). \tag{16}$$

Authors in [11] have shown that, the mean firing rate should be at least three times as large as the standard deviation of firing rate to ensure linear encoding, for which the probability that $\lambda(t)$ is negative is less than 0.01. Hence, the contrast (the coefficient of variation) of firing rate, i.e., the ratio of the standard deviation to the mean of the neural firing process, shoud be less than or equal to 1/3, i.e., $c_\lambda \leq 1/3$ condition should be satisfied. Using (11), it is clear that $\sigma_\lambda = \bar{\lambda}b\sigma_v$ as the rate, i.e., $\lambda(t)$ is linearly dependent on $v(t)$, which is a zero mean linear filtered WSS random process. Therefore, $\sigma_v \leq 1/(3b)$ is the required condition for linear encoding. Due to the linear relation between $m(t)$ and $v(t)$, we infer that

$$\sigma_v^2 = \int S_m(f) \frac{R^2}{1 + (2\pi f RC)^2}\,\mathrm{d}f \leq \left(\frac{1}{3b}\right)^2. \tag{17}$$

Hence, the variance of the presynaptic stimulus should satisfy the constraint given in (17) to ensure linear encoding.

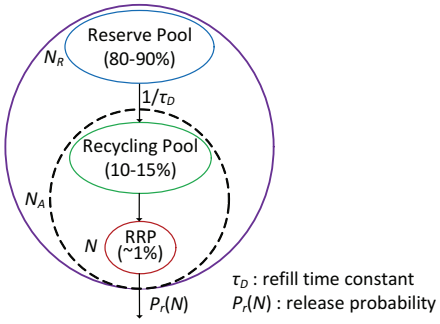

Fig. 2. The pool-based synapse model.

B. Vesicle Release Model

We use a pool-based synapse model for each presynaptic neuron to study vesicle depletion and recovery. The vesicle release process depends primarily on the vesicle pool size and postsynaptic receptor saturation [16]. In chemical synapses, some vesicles are docked at the membrane waiting to release their content upon the arrival of a trigger signal. Others are stored in the membrane pool, just above the docked vesicles, being more distant to the cell membrane. Vesicles in the neural terminal can be grouped into three sub-pools according to their relative mobilities: the readily releasable pool (RRP), the recycling pool and the reserve pool, which differ on the basis of the relative mobility of vesicles in each pool [19]. It takes the longest to mobilize the vesicles in the reserve pool while in RRP, vesicles are ready to mobilize upon arrival of a spike.

Let the pool sizes, i.e., the number of vesicles in pools, be denoted as N, $N_A - N$, and N_R, for RRP, the recycling pool and the reserve pool, respectively. N_A is the total vesicle size in the recycling pool and RRP. The recycling pool is close to the cell membrane, and tends to be cycled at moderate stimulation, so that the rate of vesicle release is the same as, or lower than, the rate of vesicle formation. Once the RRP and the recycling pool are exhausted, the reserve pool is mobilized [19]. A pool-based synapse model is illustrated in Fig. 2.

In the pool model shown in Fig. 2, $p_r(N)$ is the release probability per stimulus, and the available pool is exhausted with a rate $1/\tau_D$. Therefore, the reserve pool should recover the available, i.e., docked, pool with a time constant τ_D [16].

Release of single vesicle upon arrival of a spike is governed by a Poisson process with non-constant presynaptic firing rate $\lambda(t)$. Then, the fusion rate, i.e., the rate at which the vesicles are expelled through exocytosis [16], for a single vesicle is

$$\alpha_{v_k} = \int_0^{\Delta t_k} \lambda(t)\,\mathrm{d}t, \tag{18}$$

where the integration is evaluated over the duration of the presynaptic pulse [16]. In the calculation of α_{v_k}, we divide $\lambda(t)$ into windows of equal durations. If we choose sufficiently large number of windows of equal duration, there exists at most one spike at each window. Discretizing the fusion rate, as soon as the spike is within a specified window and the window size is small enough, the fusion rate is the same independent of at which time point the spike is. This makes sense because the fusion rate stays constant for a sufficiently small interval. This is also a realistic assumption since we need to discretize the time axis in our simulations. In (18), subscript k denotes the window index, and the integration is from the beginning of the presynaptic stimulus taken as the time origin till the end of k^{th} time window of the stimulus denoted as Δt_k.

Additional to presynaptic firing rate, the level of activation of inhibitory auto-receptors, i.e., the receptors located in the presynaptic membrane that serve as a part of a feedback loop in signal transduction by inhibiting further release or synthesis of the neurotransmitters, also affect the fusion rate [16]. Furthermore, the vesicle release probability depends on the spike-triggered Ca^{2+} influx. Therefore, the vesicle fusion rate is replaced with $\alpha_{v_k} \rightarrow \frac{\alpha_{v_k}}{(1+C_x x(t))^q}$. The constant C_x controls the strength of the inhibition, and parameter q specifies Ca^{2+} cooperativity of vesicle release [16]. However, to simplify the analysis, we ignore the effect of inhibitory auto-receptors.

Using the vesicle fusion rate defined in (18), the single-vesicle release probability is $p_{v_k} = 1 - \exp(-\alpha_{v_k})$. The release probability per stimulus is the complement of the failure probability, which is the probability that no vesicle is released during the window of interest, given by

$$p_r(N_k) = 1 - \exp(-\alpha_{v_k} N_k), \tag{19}$$

where N_k is the number of vesicles in the RRP available for release at the k^{th} window and the failure probability is $1 - p_r(N_k) = \exp(-\alpha_{v_k} N_k)$ [9]. For the more realistic case where each release site is permitted to have its own release probability, the probability that no vesicle fuses on the k^{th} interval can be calculated as $\prod_{j=1}^{N_k}(1 - p_{v_{jk}})$, where $p_{v_{jk}} = 1 - \exp\left(-\alpha_{v_{jk}}\right)$, as explicitly pointed out in [20]. Here $p_{v_{jk}}$ and $\alpha_{v_{jk}}$ are the probability that the j^{th} vesicle fuses on during k^{th} interval, and its fusion rate, respectively.

To find the mutual release probability, i.e., $p^*_{v_k}$, that gives the same result as the calculation with different release probabilities per vesicle, we set $\prod_{j=1}^{N_k}(1 - p_{v_{jk}}) = (1 - p^*_{v_k})^{N_k}$.

$$p^*_{v_k} = \frac{1}{N_k}\sum_{j=1}^{N_k} p_{v_{jk}}. \tag{20}$$

$p^*_{v_k}$ is the average release probability per vesicle for the pool of vesicles. Using the $p_{v_{jk}}$ expression and (20), the mutual fusion rate, i.e., $\alpha^*_{v_k}$, can be obtained as $\alpha^*_{v_k} = \ln(N_k) - \ln\left(\sum_{j=1}^{N_k}\exp\left(-\alpha_{v_{jk}}\right)\right)$. This equation gives a compact expression when each vesicle has a distinct fusion rate depending on the distinct release sites on presynaptic neuron, regional differences in the strength of inhibitory effects, Ca^{2+} concentration levels, and presynaptic auto-receptors.

There is some previous work concentrating on univesicular release mechanism [10]. The all-or-none synaptic transmission that arises from the saturation of postsynaptic receptors by neurotransmitter content of a single vesicle is suggested in [21], implying the same postsynaptic response regardless of the number of vesicles released. In [11], it is assumed that each action potential yields at most one vesicle release and the vesicle release process is modeled by a Z-channel because without stimuli the probability of spontaneously generated vesicles is very low, and hence, ignored. Additional to single vesicle release case, multivesicular release is studied in [16]. Moreover, it is found that the temporal correlation between stochastic responses to a repetitive train of stimuli behaves differently depending on whether multiple releases are allowed.

In univesicular release case, vesicle release at k^{th} spike arrival is bernoulli distributed with probability p_{v_k}. Hence, expected number of vesicles released at k^{th} spike is equivalent to p_{v_k}. In multivesicular release, on the other hand, each vesicle has Z-channel model with an independent (not necessarily identical) release probability, i.e, $p_{v_{jk}}$, and the average release probability is p_{v_k}, as calculated in (20). The model for multivesicular release can be represented by a non-binary Z-channel. Binary symbols of the SISO Z-channel are scaled by N_k, which is the total number of available vesicles in the RRP to be released upon spike generation at the presynaptic terminal. This assumption is valid since the vesicle release rate is scaled by N_k in multivesicular release case.

In this paper, we study multivesicular release. We model the number of vesicles released in response to an action potential exerted at k^{th} window with a random variable denoted as W_k. W_k is determined by a binomial distribution with parameters p_{v_k} and N_k. Assuming that vesicles have the same probability of release, i.e., p_{v_k}, upon a stimulus, the expected number of vesicles released on window k can be calculated as $\langle W_k\rangle = \sum_{i=0}^{N_k} iP(W_k = i) = p_{v_k}N_k$. The probability that at least one vesicle is released, the release probability, on window k is

$$P_k = 1 - (1 - p_{v_k})^{N_k}. \tag{21}$$

The release probability on the next window, i.e., P_{k+1}, can be calculated using $p_{v_{k+1}}$ and N_{k+1} by applying the iteration

$$N_{k+1} = N_k - \langle W_k\rangle + N^{rf}_{k+1} = N_k(1 - P_k)^{\frac{1}{N_k}} + N^{rf}_{k+1} \tag{22}$$

into (21), where P_k is the measured release probability for the previous, i.e., k^{th} time window, $\langle W_k\rangle$ is the average number of vesicles released on k^{th} window and N^{rf}_{k+1} is the number of vacancies in the releasable pool refilled by the reserve pool during the time difference between consecutive windows, i.e., one inter-spike interval (ISI), which can be calculated as $N^{rf}_{k+1} = N_R P^{rf}_{k+1}$. N_R and P^{rf}_{k+1} are the reserve pool size and the vesicle refill probability during one ISI, respectively. According to the derivation in [16], the reserve pool fills the vacancies with a time constant τ_D. Thus, it takes τ_D time for the system to reach $1 - 1/e$ of its final value, which is $P^{rf*}_k = 1$. Hence, provided the reserve pool size remains unchanged, the refill probability is $P^{rf}_k = 1 - \exp(-\Delta t_k/\tau_D)$, where Δt_k is the time interval between the start of the stimulus until the end of k^{th} window and τ_D is the refill time constant which is inverse of vacancy refill rate [16].

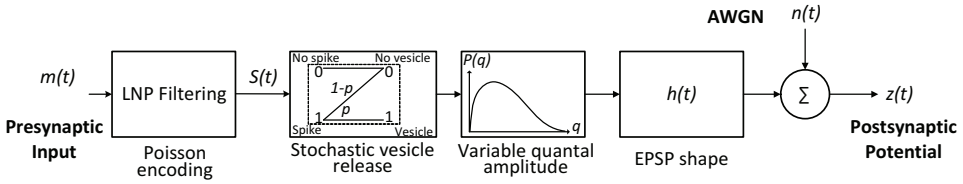

Fig. 3. Single-input single-output neuro-spike channel model between presynaptic and postsynaptic neuron terminals.

C. Postsynaptic Response with Variability in Vesicle Release

The postsynaptic response function to the release of a single vesicle is denoted by $h(t)$. Output of this response filter is subject to additive white gaussian noise denoted as $n(t)$ and the channel output is the postsynaptic voltage, i.e., $Z(t)$.

We model the postsynaptic response by $h(t)$, which corresponds to the EPSP waveform of a fast, voltage-independent AMPA-like synapse modeled as an alpha function [22],

$$h(t) = h_p \frac{t}{t_p} \exp\left(1 - \frac{t}{t_p}\right), \tag{23}$$

where h_p is the peak EPSP magnitude and t_p is the corresponding time-to-peak. The Fourier transform of $h(t)$ is $H(f) = h_p \exp(1)/t_p \left(\frac{1}{t_p} + j2\pi f\right)^2$, which is used in the rate region analysis for synaptic communication in Section III-B.

We assume that the postsynaptic responses to a sequence of vesicle releases add linearly. We incorporate synaptic variability by multiplying the response $h(t)$ by a random variable q drawn from a probability distribution $P(q)$, which can be measured empirically. q models the trial-to-trial variability in the amplitude of the postsynaptic responses observed for central neurons. In some cases, the variance in the size of EPSP is as large as the mean. Despite being possibly biased due the inability of measuring very small synaptic events, the experimentally observed amplitude distributions are usually skewed to high amplitudes and can be modeled by a Gamma distribution [23]. Here, we model $P(q)$ by a gamma distribution. A gamma-distributed random variable Q with shape α and rate β is denoted by $Q \sim \Gamma(\alpha, \beta)$. The probability density function (pdf) of Q is

$$\mathrm{f}(q; \alpha, \beta) = \beta^{\alpha} \frac{1}{\Gamma(\alpha)} q^{\alpha-1} \exp(-\beta q),\ q \geq 0,\ \alpha, \beta > 0, \tag{24}$$

where α is the order of the distribution. If α is a positive integer, then $\Gamma(\alpha) = (\alpha - 1)!$. The mean $\bar{q}$, standard deviation σ_q and the coefficient of variation of the gamma distribution are defined as $\bar{q} = \alpha/\beta$, $\sigma_q = \alpha/\beta^2$ and $c_q = 1/\beta$, respectively. Here, we choose $\alpha = \beta = 0.6^{-1}$, consistent with the postsynaptic quantal variation, i.e., the variation in the transmitter content among vesicles, model proposed in [11].

Four parameters are thought to be particularly important in determining trial-to-trial EPSC variability: the time course and probability of quantal release, i.e., the amount of neurotransmitter released following neural stimulation, the number of release sites, where the secretion of a quantum of neurotransmitter occurs, and the quantal size, which is the postsynaptic response to the release of neurotransmitter from a single vesicle [24]. Although in [24], authors claim that multivesicular release can cause postsynaptic saturation, i.e., full receptor occupancy, here, we assume that receptors at the postsynaptic terminal are not saturated by multivesicular release assuming the available number of postsynaptic receptors is high enough.

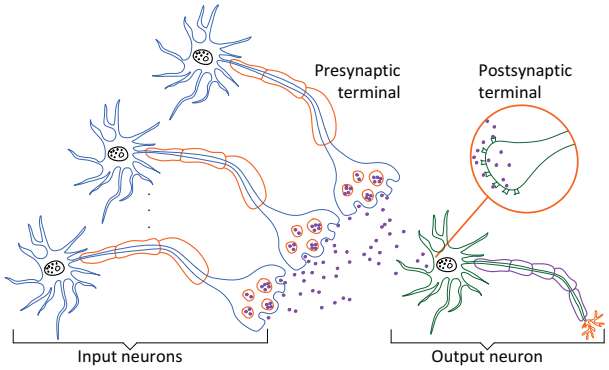

Fig. 4. Multiple-access synaptic communication channel model.

The postsynaptic membrane voltage is

$$Z(t) = \sum_{l=1}^{M} \sum_{i} q_i^l W_i^l h^l(t - t_i) + n(t), \tag{25}$$

where q is the random EPSP amplitude and W is a binomial variable representing the spike-conditioned vesicle release process. Superscript l refers to the l^{th} synaptic connection. If the synapses are distributed at different electrotonic locations, i.e., positions along the excitable cell with unequal electrical state in the absence of repeated action potentials, on the postsynaptic neuron, the corresponding EPSP waveforms $h^l(t)$ are different [11]. In this paper, we assume that synaptic connections are at the same electrotonic location, and hence, they are identical and have the same EPSP characteristics.

Assuming a point-to-point synaptic connection between a pre- and postsynaptic neuron terminal pair, the postsynaptic membrane voltage can be calculated as

$$Z(t) = \left[h(t) * \sum_{i} q_i W_i \delta(t - t_i) \right] + n(t), \tag{26}$$

where W_i is a binomial random variable representing the spike-conditioned vesicle release process to a spike generated at t_i^{th} time instant. If the spike generated at time t_i does not lead to vesicle release at input neurons, $W_i = 0$. The model for the SISO neuro-spike channel model is given in Fig. 3. In Section III, we extend the single-input synaptic model to multi terminal input case, and investigate its rate region.

III. Multiple-Access Neuron Channel

We extend the SISO channel model to MISO, i.e., multiple-access, channel model. We assume that presynaptic terminals

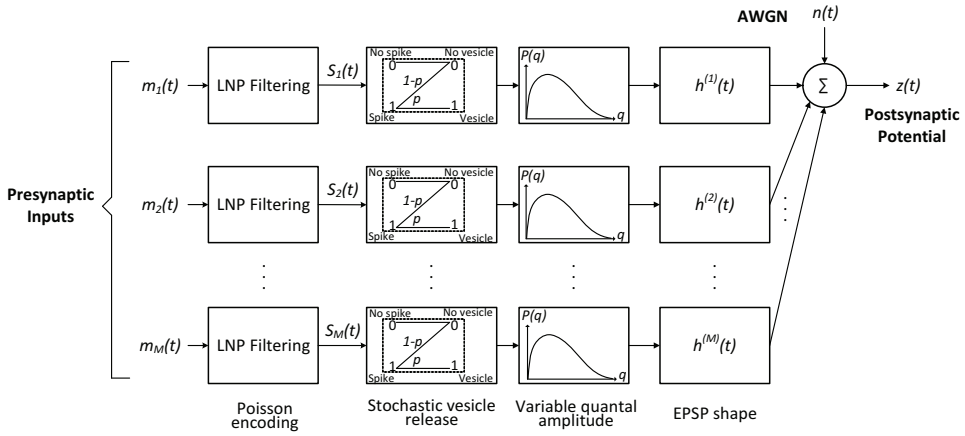

Fig. 5. Multiple-access channel model between presynaptic and postsynaptic neuron terminals.

are identical, i.e., the axons share the LNP model features and spike generation mechanisms, and the EPSP characteristics are the same. A conceptual model for the multiple-access synaptic communication channel is illustrated in Fig. 4.

In Fig. 5, the hypothetical model for multiple-access channels among neuron terminals is illustrated. Upon arrival of the spike train, the presynaptic terminals independently release vesicles with an average probability of p. The released vesicles are directed to a common postsynaptic terminal through distinct synapses with separate input terminals. In this paper, we assume that the synaptic impulse responses, i.e., the EPSP characteristics, are identical in shape. However, each synaptic channel is characterized by a random amplitude determined by a Gamma distributed variable q. Hence, the synaptic channels can be independently characterized. At the end of the transmission, voltage seen at the postsynaptic terminal is stochastically determined by the random spike generation and vesicle release processes at each input terminal, and the variabilities at each synaptic channel. In this section, we analyze the rate region for multiple-access synaptic communication channel.

A. Modulated Input Power Spectral Density

Using the approximation for the spike train PSD in (16),

$$S_s(f) \approx \bar{\lambda} + \left(\bar{\lambda}b\right)^2 |K(f)|^2 S_m(f) + \bar{\lambda}^2 \delta(f) \tag{27}$$

$$\sigma_\lambda^2 = \int \left[\left(\bar{\lambda}b\right)^2 |K(f)|^2 S_m(f) + \bar{\lambda}^2 \delta(f)\right] \mathrm{d}f. \tag{28}$$

Similar to spike generation process, the vesicle release process is also Poisson with rate $p_{v_k} N_k \lambda(t)$. Thus, the PSD for vesicle release process at k^{th} window, i.e., $S_w^{(k)}$, can be obtained as

$$\begin{aligned} S_w^{(k)}(f) &= \left(p_{v_k} N_k\right)^2 \left[\left(\bar{\lambda}b\right)^2 |K(f)|^2 S_m(f) + \bar{\lambda}^2 \delta(f)\right] \\ &+ \left(p_{v_k} N_k\right) \bar{\lambda}. \end{aligned} \tag{29}$$

Next, by considering the effect of channel variability, represented by the random variable q, we define $S_l^{(k)}(f)$ as the PSD of the modulated input l at k^{th} window of interest. Here, modulated input is the presynaptic neuron stimulus passing through LNP filter to be Poisson encoded, and converted into binomial vesicle release form and then scaled with random quantal amplitude to be filtered with postsynaptic response function. Modulated input is a function of frequency and random due to the stochastic variables denoting vesicle release and synaptic filter amplitude.

$$\begin{aligned} S_l^{(k)}(f) &= \bar{q}^2 \left(p_{v_k} N_k\right)^2 \left[\left(\bar{\lambda}_l b\right)^2 |K(f)|^2 S_{m_l}(f) + \left(\bar{\lambda}_l\right)^2 \delta(f)\right] \\ &+ \left(\bar{q}^2 + \sigma_q^2\right) \left(p_{v_k} N_k\right) \bar{\lambda}_l, \end{aligned} \tag{30}$$

following from (29), the linear encoding restriction and the approximation of $Var(qp\lambda_l(t))$ as

$$\begin{aligned} Var(qp\lambda_l(t)) &= \mathrm{E}\left[q^2 \left(p_{v_k} N_k\right)^2 \lambda_l^2(t)\right] - \bar{q}^2 \left(p_{v_k} N_k\right)^2 \bar{\lambda}_l^2 \\ &= \left(\bar{q}^2 + \sigma_q^2\right) \left(p_{v_k} N_k\right)^2 \sigma_{\lambda_l}^2 \\ &+ \left(\bar{q}^2 + \sigma_q^2\right) \left(p_{v_k} N_k\right)^2 \bar{\lambda}_l^2 - \bar{q}^2 \left(p_{v_k} N_k\right)^2 \bar{\lambda}_l^2 \\ &\approx \sigma_q^2 \left(p_{v_k} N_k\right)^2 \bar{\lambda}_l^2 + \bar{q}^2 \left(p_{v_k} N_k\right)^2 \sigma_{\lambda_l}^2. \end{aligned} \tag{31}$$

Approximation in (31) follows from that the mean firing rate is at least three times larger than the standard deviation of firing rate to ensure linear encoding [11]. Hence, $c_\lambda = \sigma_\lambda / \bar{\lambda} \leq 1/3$ should be satisfied, and the $\sigma_q^2 \left(p_{v_k} N_k\right)^2 \sigma_{\lambda_l}^2$ term is negligible.

From (31), variability of q only affects the frequency independent part of the modulated input, i.e., the term $(p_{v_k} N_k)\bar{\lambda}_l$ in (29), due to linear encoding condition. As a result, the variation at the frequency dependent part is ignored.

For single synapse channel, the power spectrum of $z(t)$ can be calculated as in [11], i.e.,

$$S_Z(f) = |H^{(l)}(f)|^2 S_l^{(k)}(f) + S_n(f). \tag{32}$$

Extending this model to multiple input case for M number of presynaptic neurons, we obtain

$$S_Z(f) = \sum_{l=1}^{M} |H^{(l)}(f)|^2 S_l^{(k)}(f) + S_n(f). \tag{33}$$

B. Multiuser Channel Rate Regions

The multiaccess coding theorem (MACT) asserts that if source l, $1 \leq l \leq M (l \geq 2)$ has rate R_l and is constrained to a PSD S_l over the given bandwidth B, then, arbitrarily small error probability can be achieved for all sources if for each

subset $A \subseteq \{1, 2, \ldots, M\}$ [25],

$$\sum_{l \in A} R_l < \int_{-B/2}^{B/2} \log \left(1 + \frac{\sum\limits_{l \in A} S_l |H^{(l)}(f)|^2}{N_0} \right) \mathrm{d}f, \qquad (34)$$

where $H^{(l)}(f)$ is the Fourier transform of $h^{(l)}(t)$. The quantity on the right hand side of (34) is the conditional average mutual information per unit time, $I(A)$, between the inputs in A and the output, conditional on the inputs not in A. This assumes that the inputs are independent stationary white Gaussian noise processes over the bandwidth B. From MACT,

$$\sum_{l \in A} R_l < \max_{S_l^{(k)}(f)} \int_{-B/2}^{B/2} \log \left(1 + \frac{\sum\limits_{l \in A} |H^{(l)}(f)|^2 S_l^{(k)}(f)}{N_0} \right) \mathrm{d}f$$

$$\text{s.t.} \sum_{l \in A} \int S_l^{(k)}(f)\, \mathrm{d}f \leq \sum_{l \in A} P_l^{(k)}, \qquad (35)$$

for multiple input synaptic communication channel, where $P_l^{(k)}$ is the power constraint of the l^{th} presynaptic neuron over the bandwidth B, and $A \subseteq \{1, \ldots, M\}$ is the input subset.

IV. Performance Evaluation

In this section, we evaluate the analytical expressions obtained in Sections II-III. The numerical parameters, as tabulated in Table I, are obtained from [9], [11], [18].

Initially, we generate spike trains using the LNP model with $\lambda_{\max} = 36.03$ Hz as discussed in Section II-A. We apply a normal distributed stimulus to each presynaptic neuron terminal. The outputs of the LNP filters, i.e., the generated spike trains based on the firing rates are illustrated in Fig. 6.

Spike trains, i.e, action potentials, are converted into the form of vesicle release. Rate of the spike trains determines the triggering level for vesicle release mechanism. During each repetition of the train, the RRP decreases by 1 each time a vesicle is released. The release probability at a synapse is directly correlated with the size of its readily releasable vesicle pool, which is N. In [9], authors choose $N_A = 3-10$ in their simulations. For the vesicle refill time constant they use a value of $\tau_D = 2$ s, which agrees with the time of recovery of the RRP measurements in hippocampal slice experiments. Therefore, we choose the refill rate and reserve pool size based on these experiments. The simulation result for the dynamic vesicle release process, which is initiated with the spike train given in Fig. 6 with $\mathrm{E}[\lambda] = 15.84$, is depicted in Fig. 7.

Passing through the synaptic channel, the released molecules are modulated. Modulation is due to the variability in the number of available receptors on the surface of the postsynaptic neuron. Furthermore, the synaptic channel behaves like an alpha-shaped filter, the input and the output of which are the modulated input and the postsynaptic potential observed at the destination neuron, respectively. A segment of a typical EPSP waveform is shown in Fig. 8.

We observe the vesicle release probability during a spike train to characterize how the average rate per spike varies. We analyze the fusion rate by dividing the spike train into 100 windows of equal duration. As fusion rate, i.e, α_v, is solely dependent on the integration duration of $\lambda(t)$, it increases during train as seen in Fig. 9(a). Furthermore, the average vesicle release probability, i.e., p_v, also increases with α_v, agreeing with the results obtained in [20]. Therefore, average number of vesicles released increases during train, which is illustrated in Fig. 9(b). Hence, the information rate is also augmented with impulse train duration as shown in Fig. 9(c).

TABLE I
Analysis parameters.

Parameter	Symbol	Value / Range
Soma time constant	$\tau = RC$	20 ms
AWGN bandwidth	B_n	100 Hz
AWGN standard deviation	σ_n	0.1 mV
Peak magnitude of the EPSP waveform	h_p	1 mV
Time at which EPSP reaches its peak	t_p	0.5 ms
Firing rate control parameter	a	$1/0.029^\circ$
Voltage at half the maximum firing rate	$v_{1/2}$	0.036°
The vesicle release probability	p_{v_k}	0.4
Average firing rate	α_{v_k}	10 $spikes$/s
Available and reserve pool sizes	N_A, N_R	$3-10, 60$
Vesicle refill time constant	τ_D	2 s
Quantal amplitude mean and CV	$\bar{q}, c_q$	1, 0.6

As the presynaptic firing rate enhances, the information bits delivered per spike increases. Making realistic assumptions on the rate of spike trains, authors in [9] come across the typical spike rate of neurons, which is 1 spike per 100 ms. Therefore, we limit $\lambda(t)$ to be around this typical value in our simulations. Using (35), we can obtain the rate region for SISO neuro-spike communication channel. The rate region for varying RRP size, i.e., N_A, and reserve pool size, i.e, N_R, and vesicle refill time constant, i.e., τ_D, is pointed out in Fig. 10. As N_A increases the available number of vesicles ready for release gets higher. For larger N_R, since the refill rate gets larger, size of the available pool gets larger during the stimulus, causing improved rate values at the postsynaptic terminal. As τ_D increases, as more time is required to fill the docked pool, the docked pool depletes faster, and the rate drops.

Although in [26], authors calculate that the maximum amount of information that can be transmitted by an ideal synapse is approximately equal to 1.13 bits per spike, their analysis is based on unitary vesicle release. In this paper, as we allow multivesicular release, higher information rates become possible. We hypothetically show that rate is affected by firing of presynaptic terminal, vesicle pool sizes and refill process, vesicle fusion rate and postsynaptic receptors. Furthermore, in this study, the saturation of postsynaptic receptors, which, in fact, adversely influences the release process, is ignored. The model could be extended to observe the feedback relationship between the postsynaptic receptors and vesicle release process.

Extension of the model to multiple-access neuro-spike channel is the next step. Using (35), we can obtain the rate upper bounds for any user subset $A \subseteq \{1, \ldots, M\}$. Depending on whether the set of users has correlation among them or not, in this section, we investigate the rate regions.

Assume that M neurons are fired with an input vector $\underline{m}(t) = \{m_1(t), ..., m_M(t)\}$, and neurons release their vesicles into the synaptic channel. We analyze the sum rate regarding the dependence of the individual presynaptic neurons.

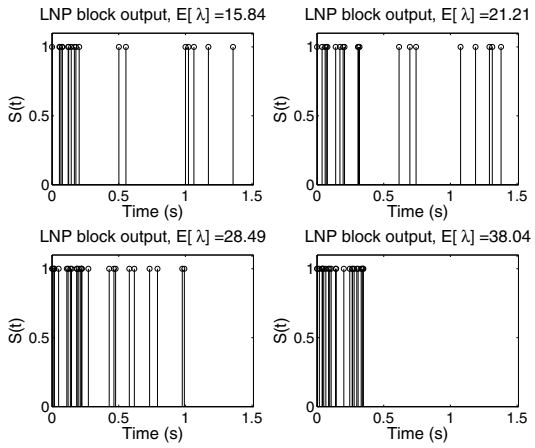

Fig. 6. The spike train at the output of the LNP filter for varying firing rates.

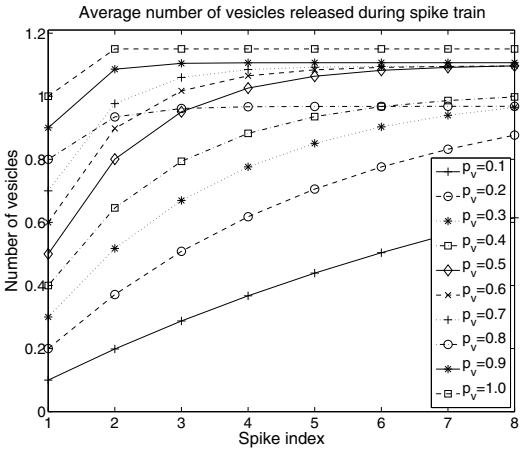

Fig. 7. Random vesicle release process in the course of Poisson spike train.

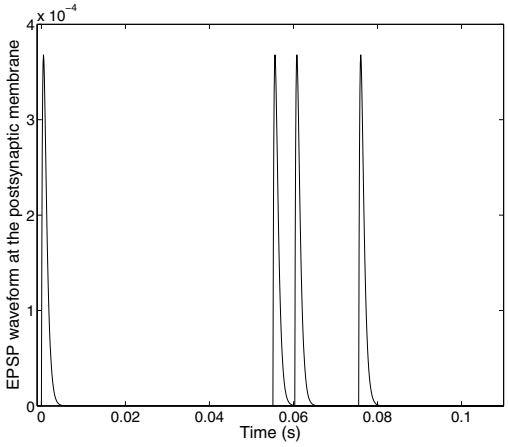

Fig. 8. EPSP waveform at the postsynaptic membrane, $\mathrm{E}[\lambda] = 15.84$.

1) Independent Firing of Neurons: Let $S_l \sim Pois(\lambda_l)$, for $l \in \{1, \ldots, M\}$ be an inhomogeneous and independent Poisson process with rate $\lambda_l(t)$ corresponding to the model of spike generation at l^{th} input neuron. The probability mass function (pmf) of S_l is given by

$$\mathrm{f}(k; \lambda_l(t)) = P(S_l = k) = \frac{\lambda_l^k(t)}{k!} \exp\left(-\lambda_l(t)\right), \; k \in \mathbb{Z}_{\geq 0}. \tag{36}$$

We define a new random process S, denoting the sum of individual independent but not necessarily identically distributed random processes S_l, i.e., S$= \sum_{l=1}^{M} S_l$. The pmf $P(S) = P(S_1 = k_1, S_2 = k_2, \ldots, S_M = k_M)$ is given by

$$P(S) = \prod_{l=1}^{M} \frac{\lambda_l^{k_l}}{k_l!} \exp\left(-\lambda_l\right) = \exp\left(-\sum_{l=1}^{M} \lambda_l\right) \prod_{l=1}^{M} \frac{\lambda_l^{k_l}}{k_l!}. \tag{37}$$

In independent firing of neurons, l^{th} neuron releases vesicles with rate $\lambda_l(t)$ independent of other neurons. Therefore, at the l^{th} input neuron, the vesicle release probability is determined by a Poisson distribution with a rate parameter $\lambda_l(t)p$, where $p = p_{v_k} N_k$ at k^{th} window of interest. Let X_l be the random process modeling the vesicle release at l^{th} input neuron. Hence, $X_l \sim Pois(\lambda_l(t)p)$, for $l \in \{1, \ldots, M\}$ independently vesicle releasing input neurons.

The vesicles released by all input neurons are accumulated at the synaptic channel. Therefore, the total vesicle release to the synaptic channel can be determined by the process $X = \sum_{l=1}^{M} X_l$, the rate of which is $\sum_{l=1}^{M} \lambda_l(t)p = p\sum_{l=1}^{M} \lambda_l(t) = p\lambda(t)$, where $\lambda(t) = \sum_{l=1}^{M} \lambda_l(t)$. Therefore, the vesicle release process can be modeled by a Poisson distribution, $X \sim Pois\left(p \sum_{i=1}^{M} \lambda_l(t)\right)$.

Under independently firing of presynaptic neurons, Fig. 11(a) illustrates the rate region for a subset $A \subseteq \{1, \ldots, M\}$ of $M = 35$ user synaptic multiple-access channel determined by (35). As shown in Fig. 11(a), the total rate does not scale with the same order as the raise in the number of users as the synaptic communication channel experiences interference.

2) Correlated Firing of Neurons: Let $T_l \sim Pois(\theta_l)$, for $l \in \{1, \ldots, M\}$ are independent random variables. Consider the random variables $S_l = T_l + T_0$, $\forall l \in \{1, \ldots, M\}$. Then, $\{S_1, S_2, \ldots, S_M\}$ jointly follow a multivariate Poisson distribution [27]. The joint pmf $P(S)$ is given by

$$P(S) = \exp\left(-\sum_{l=1}^{M} \theta_l\right) \prod_{l=1}^{M} \frac{\theta_l^{k_l}}{k_l!} \sum_{l=0}^{k_{\min}} \prod_{j=1}^{M} \binom{k_j}{l} l! \left(\theta_0 / \prod_{l=1}^{M} \theta_l\right)^l, \tag{38}$$

where $k_{\min} = \min(k_1, k_2, \ldots, k_M)$. Marginally, each presynaptic input S_l follows a Poisson distribution with rate parameter $\theta_l + \theta_0$. Therefore, $\mathrm{E}[S_l] = \theta_l + \theta_0$, and $Var[S_l] = \theta_l + \theta_0$. The correlation coefficient between S_i and S_j, i.e., ρ_{ij}, is

$$\rho_{ij} = corr(S_i, S_j) = \begin{cases} \frac{\theta_0}{\sqrt{(\theta_i+\theta_0)}\sqrt{(\theta_j+\theta_0)}} & \text{if } i \neq j \\ 1 & \text{if } i = j \end{cases}. \tag{39}$$

θ_0 is the covariance between all the pairs of random variables. In this paper, we assume common covariance for all pairs, which is a simple yet powerful conjecture enough to demonstrate the improvement in additive rate compared to the case where presynaptic inputs are uncorrelated.

In correlated firing of neurons, l^{th} neuron releases vesicles with rate $\lambda_l(t) = \theta_l + \theta_0$, where θ_0 denotes the common correlation parameter between any two neurons. At the l^{th} input neuron, the vesicle release probability is determined by

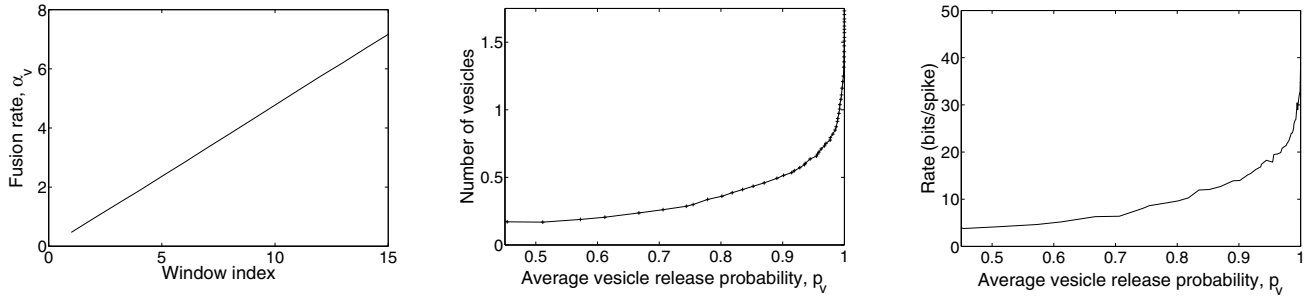

(a) (b) (c)

Fig. 9. Time dependent neuronal (a) vesicle fusion rate, (b) vesicle release process, and (c) average rate during spike train.

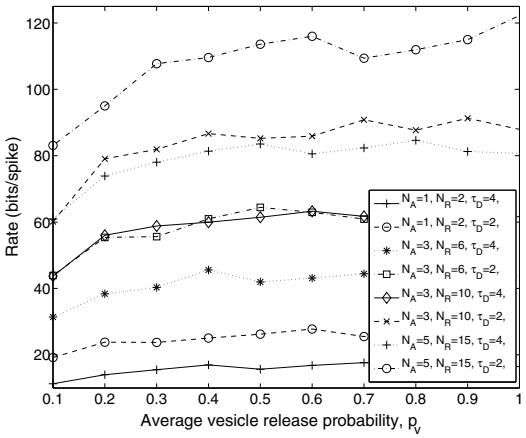

Fig. 10. The achievable rate region for SISO synaptic communication channel under variable vesicle pool conditions.

a Poisson distribution with a rate parameter $(\theta_l + \theta_0)\, p$, where $p = p_{v_k} N_k$. Let X_l be the random process modeling the vesicle release at l^{th} input neuron. Hence, in correlated firing of presynaptic neurons, the vesicle release process at l^{th} presynaptic terminal can be modeled by $X_l \sim Pois\left((\theta_l + \theta_0)\, p\right)$.

The vesicles released by all input neurons are accumulated at the synaptic channel. Therefore, the total vesicle release to the synaptic channel can be determined by the process $X = \sum_{l=1}^{M} X_l = p \sum_{l=1}^{M} T_l + pMT_0$, the rate of which is $\sum_{l=1}^{M} (\theta_l + \theta_0)\, p = p \sum_{l=1}^{M} (\theta_l + \theta_0) = p\theta + pM\theta_0$, where $\theta = \sum_{l=1}^{M} \theta_l$. Since T_l s are independent of each other, $\sum_{l=1}^{M} T_l$ has a Poisson distribution with rate parameter $\sum_{l=1}^{M} \theta_i$, which is independent from the rate coming from distribution of MT_0. However, it is nontrivial to characterize the pdf of X because MT_0 is not Poisson distributed.

Fig. 11(b) illustrates the rate region for $M = 5$ user synaptic multiple-access channel determined by (35) given that users' firing rates have first-order correlation. Since the transmitted information bits per spike remains the same independent of the correlation amount, we scale the delivered information per spike by spike count in a second, and obtain the rate as information bits per second. Compared to uncorrelated firing of neurons, the curve corresponding to $\rho = 0$, as the firing rates become more correlated, total rate in bits per second enhances. Hence, incorporating correlation, more information is conveyed through synapses to the postsynaptic end.

V. Conclusion

In this paper, we investigate the rate region for SISO synaptic communication channel model, and observe the time course of postsynaptic firing rate, and its dependence on dynamics of vesicle release process and docked pool features. Furthermore, we extend the single terminal model to multiple-access synaptic communication channel model and observe how the total information rate adds up. Moreover, we analyze the contribution of first-order correlation on the information rate at the postsynaptic neuron terminal. Our analysis puts forth the boosting effect of spike correlation on the postsynaptic rate. Open issues include investigating the disorders characterized by pre- and postsynaptic and synaptic abnormalities, and then revealing the potential relations between neuronal coefficients and disorders. The analysis could be extended to observe the effect of multi-order correlations among presynaptic terminals on the postsynaptic performance.

References

[1] I. F. Akyildiz *et al.*, "Nanonetworks: a new communication paradigm," *Computer Networks*, vol. 52, pp. 2260–2279, Aug. 2008.

[2] T. Nakano *et al.*, "Molecular communication for nanomachines using intercellular calcium signaling," in *Proc. 2005 IEEE Conference on Nanotechnology*, pp. 478–481.

[3] M. Gregori and I. F. Akyildiz, "A new nanonetwork architecture using flagellated bacteria and catalytic nanomotors," *IEEE J. Sel. Areas Commun.*, vol. 28, no. 4, pp. 612–619, 2010.

[4] M. Kuscu and O. B. Akan, "A physical channel model and analysis for nanoscale molecular communications with Forster resonance energy transfer (FRET)," *IEEE Trans. Nanotechnol.*, vol. 11, pp. 200–207, 2012.

[5] L. Parcerisa and I. F. Akyildiz, "Molecular communication options for long range nanonetworks," *Computer Networks J.*, vol. 53, no. 16, pp. 2753–2766, Nov. 2009.

[6] A. L. Hodgkin and A. F. Huxley, "A quantitative description of membrane current and its application to conduction and excitation in nerve," *J Physiol.*, vol. 117, no. 4, pp. 500–544, Aug. 1952.

[7] E. Balevi and O. B. Akan, "A physical channel model of nanoscale neurospike communication," to appear in *IEEE Trans. Commun.*, 2013.

[8] J. P. Meeks and S. Mennerick, "Action potential initiation and propagation in CA3 pyramidal axons," *J Neurophysiol.*, vol. 97, pp. 3460–3472, 2007.

[9] L. E. Dobrunz and C. F. Stevens, "Heterogeneity of release probability, facilitation, and depletion at central synapses," *Neuron*, vol. 18, pp. 995–1008, Jun. 1997.

[10] C. F. Stevens and Y. Wang, "Facilitation and depression at single central synapses," *Neuron*, vol. 14, pp. 795–802, Apr. 1995.

[11] A. Manwani and C. Koch, "Detecting and estimating signals over noisy and unreliable synapses: information-theoretic analysis," *Neural Comput.*, vol. 13, no. 1, pp. 1–33, Jan. 2001.

[12] M. Bartos *et al.*, "Synaptic mechanisms of synchronized gamma oscillations in inhibitory interneuron networks," *Nat. Rev. Neurosci.*, vol. 8, pp. 45–56, Jan. 2007.

[13] B. W. Connors and M. A. Long, "Electrical synapses in the mammalian brain," *Annu. Rev. Neurosci.*, vol. 27, pp. 393–418, Jul. 2004.

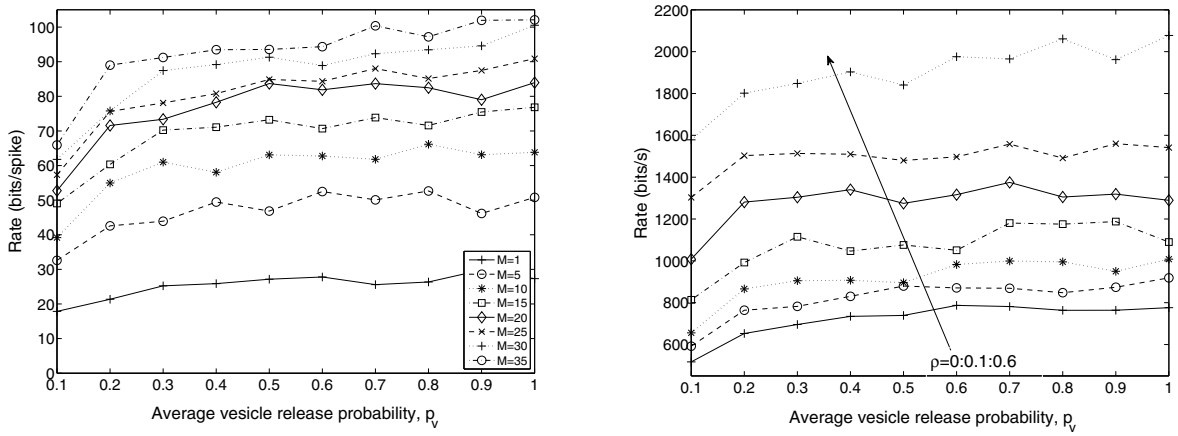

(a) (b)

Fig. 11. (a) The rate region for multiple-access synaptic communication channel under independent firing of presynaptic neurons for a subset $A \subseteq \{1, \ldots, M\}$ of $M = 35$ presynaptic terminals, and (b) correlated firing of presynaptic neurons for $M = 5$ presynaptic terminals with $\rho = 0 : 0.1 : 0.6$.

[14] M. C. W. van Rossum and G. G. Turrigiano, "Correlation based learning from spike timing dependent plasticity," *Neurocomputing*, vol. 38–40, pp. 409–415, Jun. 2001.

[15] A. Guney, B. Atakan, and O. B. Akan, "Mobile ad hoc nanonetworks with collision-based molecular communication," *IEEE Trans. Mobile Computing*, vol. 11, no. 3, pp. 353–266, Mar. 2012.

[16] V. Matveev and X.-J. Wang, "Implications of all-or-none synaptic transmission and short-term depression beyond vesicle depletion: a computational study," *J. Neurosci*, vol. 20, no. 4, pp. 1575–1588, Feb. 2000.

[17] E. P. Simoncelli, L. Paninski, J. Pillow, and O. Schwartz, "Characterization of neural responses with stochastic stimuli," in *The New Cognitive Neurosciences,* M. Gazzaniga, editor. MIT Press, 2004.

[18] P. Dayan and L. F. Abbott, Theoretical Neuroscience: Computational and Mathematical Modeling of Neural Systems. MIT Press, 2001.

[19] S. O. Rizzoli and W. J. Betz, "Synaptic vesicle pools," *Nature Reviews Neuroscience*, vol. 6, pp. 57–69, Jan. 2005.

[20] L. E. Dobrunz, "Release probability is regulated by the size of the readily releasable vesicle pool at excitatory synapses in hippocampus," *Int. J. Devl Neuroscience*, vol. 20, pp. 225–236, 2002.

[21] C. M. Tang *et al.*, "Saturation of postsynaptic glutamate receptors after quantal release of transmitter," *Neuron*, vol. 13, pp. 1385–93, Dec. 1994.

[22] W. Rall, "Distinguishing theoretical synaptic potentials computed for different soma-dendritic distributions of synaptic input," *J. Neurophysiol.*, vol. 30, pp. 1138–1168, 1967.

[23] J. M. Bekkers *et al.*, "Origin of variability in quantal size in cultured hippocampal neurons and hippocampal slices," in *Proc. Natl. Acad. Sci. USA*, vol. 87 no. 14, pp. 5359–5362, Jul. 1990.

[24] P. B. Sargent *et al.*, "Rapid vesicular release, quantal variability, and spillover contribute to the precision and reliability of transmission at a glomerular synapse," *J. Neurosci*, vol. 25, no. 36, pp. 8173–8187, Sep. 2005.

[25] R. G. Gallager, "An inequality on the capacity region of multiaccess multipath channels," in *Communications and Cryptography: Two Sides of One Tapestry*, R. E. Blahut, D. J. Costello Jr., U. Maurer, and T. Mittelholzer, editors. Kluwer, 1994, pp. 129–139.

[26] F. Gabbiani and C. Koch, "Coding of time-varying signals in spike trains of integrate-and fire neurons with random threshold," *Neural Comput.*, vol. 8, pp. 44–66, 1996.

[27] T. Brijs *et al.*, "A multivariate Poisson mixture model for marketing applications," *Stat Neerl*, vol. 58, no. 3, pp. 322–348, 2004.

Derya Malak [S'11] (dmalak@ku.edu.tr) received her B.Sc. degree in Electrical and Electronics Engineering from Middle East Technical University, Ankara, Turkey, in 2010. She is currently a research assistant in the Next-generation and Wireless Communication Laboratory and received her M.Sc. degree at the Department of Electrical and Electronics Engineering, Koc University. Her current research interests include nanoscale and intra-body molecular communications, and network information theory.

Ozgur B. Akan [M'00-SM'07] (akan@ku.edu.tr) received his Ph.D. degree in electrical and computer engineering from the Broadband and Wireless Networking Laboratory, School of Electrical and Computer Engineering, Georgia Institute of Technology in 2004. He is currently a full professor with the Department of Electrical and Electronics Engineering, Koc University and the director of the Next-generation and Wireless Communications Laboratory. His current research interests are in wireless communications, nano-scale and molecular communications, and information theory. He is an Associate Editor of IEEE TRANSACTIONS ON VEHICULAR TECHNOLOGY, *International Journal of Communication Systems* (Wiley), and *Nano Communication Networks Journal* (Elsevier). He served as General Co-Chair of ACM MOBICOM 2012, IEEE MoNaCom 2012, and TPC Co-Chair of IEEE ISCC 2012.